Hindawi Publishing Corporation
Journal of Nanomaterials
Volume 2015, Article ID 685323, 9 pages
http://dx.doi.org/10.1155/2015/685323

Research Article

In Vitro Hemocompatibility and Cytotoxicity Evaluation of Halloysite Nanotubes for Biomedical Application

Hao-Yang Liu,[1] Lei Du,[2] Yan-Teng Zhao,[1] and Wei-Qun Tian[1]

[1]*Department of Biomedical Engineering, School of Basic Medical Science, Wuhan University, Wuhan 430071, China*
[2]*Oil and Gas Fire Protection Key Laboratory of Sichuan Province, China Petroleum Engineering Co. Ltd. South-West Company, Chengdu 610041, China*

Correspondence should be addressed to Wei-Qun Tian; tian_weiqun@whu.edu.cn

Received 22 July 2015; Revised 17 October 2015; Accepted 19 October 2015

Academic Editor: Pingmei Guo

Halloysite nanotubes (HNTs), due to their unique structures and properties, may play an important role in biomedical applications. In vitro test is usually conducted as a preliminary screening evaluation of the hemocompatibility and cytotoxicity of HNTs for its short term consuming, convenience, and less expense. In this work, HNTs were processed with anticoagulated rabbit blood to detect its blood compatibility. The result of hemolysis test shows that the hemolysis ratios are below 0.5%, indicating nonhemolysis of HNTs. Plasma recalcification time suggests that HNTs are dose-dependently contributing to blood coagulation in platelet poor plasma (PPP). The effect of platelet activation caused by HNTs was also examined by scanning electron microscopy (SEM). Meanwhile, HNTs were labeled with fluorescein isothiocyanate (FITC) to observe its intracellular distribution in A549 cells under confocal microscopy. CCK-8 test and TUNEL test of HNTs at different concentration levels were performed in vitro, respectively. Therefore, the potential usage of HNTs in medicine may be very meaningful in oral dosing, dermal application, dental uses, or medical implants.

1. Introduction

As a kind of naturally occurring nanomaterial, HNTs have obtained extensive research because of its distinctive tubular morphology and natural abundance. Halloysite nanotubes ($Al_2Si_2O_5(OH)_4 \cdot nH_2O$) are layered aluminosilicate material, with unique cylindrical structure and high aspect ratio [1–3]. HNTs are of the length of 0.5–1.5 μm, the inner diameter of 10–40 nm, and the outer diameter of 40–70 nm, respectively. The outermost surface of HNTs possesses similar chemical properties of SiO_2, while the inner tubular surface is chemically similar to those of Al_2O_3 [3–7]. In recent years, considerable studies have been done to explore new application of HNTs in different fields, such as polymer nanocomposites [8–13], thermal resistance [14–16], and antifouling [17–21]. Moreover, there has also been lots of interest in utilizing the properties of HNTs for promising biomedical applications.

Several experiments have been performed on interactions between HNTs and living cells or tissues. Fakhrullina et al. analysed the nanosafety of halloysite for soil nematodes, and they concluded that HNTs suggest a low toxicity to soil nematodes and are likely to be environmentally safe [22]. Liu et al. combined HNTs and chitosan to prepare a novel tissue engineering scaffold [23]. According to the authors, mouse fibroblasts can attach to the composites readily and it exhibits great potential for applications in tissue engineering or as drug/gene carriers. Lvov et al. reported the application of HNTs as a drug delivery vehicle, and they further confirmed that the drug release rate could be controlled by coating polymers onto the drug loaded HNTs [24]. Hughes and King performed a study to evaluate the feasibility of HNTs-based composites to capture leukemic cells under flow, which provide a practical route for enhancing cancer cell capture [25]. Also, the possibility of applying PLA-HNTs composites for bone implants was reported [26]. The utilizing of the advantages of HNTs in biomedical field, particularly their cylindrical shape and their excellent mechanical properties, relies heavily on their biocompatibility. Although the above-mentioned studies have investigated some biological system

responses to HNTs and several standard biocompatibility assays are ongoing, the information addressing potential risk related to HNTs exposure still should be taken seriously. In particular, the genotoxicity for living cells and blood compatibility of HNTs have not been demonstrated yet.

In the present work, HNTs were labeled with FITC and were imaged under confocal microscopy to observe its distribution inside A549 cells. CCK-8 assay and TUNEL test were performed to examine the cell viability and genotoxicity of HNTs. Hemolysis test, plasma recalcification test, and platelet activation test were carried out, respectively, with anticoagulated rabbit blood to probe the blood compatibility of HNTs. These results provide a more comprehensive evaluation of HNTs and will be pretty useful for its further application.

2. Materials and Methods

2.1. Materials. HNTs were obtained from Jin Yang Guang Ceramic Co. Ltd. (Zhengzhou, China). Fluorescein isothiocyanate isomer I (FITC) and aminopropyl triethoxysilane (APTES) were purchased from Sigma-Aldrich. Hoechst 33342, DiD, and cellulose ester membranes (dialysis bag) were purchased from Beyotime Biotechnology Co. Ltd. (Nantong, China). Fetal bovine serum (FBS), DMEM, trypsin/EDTA, and penicillin-streptomycin were purchased from Hyclone Co. (South Logan, UT). Purified deionized water prepared by Milli-Q system (Millipore Co., Billerica, MA, USA) was used to prepare all of the solutions. All other chemicals and regents were of analytical grade and used as received.

2.2. Cell Culture. A549 (human Caucasian lung carcinoma) cells were cultured in DMEM supplemented with 10% (vol/vol) FBS, penicillin (100 μg/mL), and streptomycin (100 μg/mL). All the cells were maintained in a humidified 5% CO_2 atmosphere at 37°C.

2.3. Fluorescence Labeling. HNTs were purified with a typical procedure [27]. A 10 wt% water solution of HNTs was prepared to dry halloysite. Then 0.05 wt% sodium hexametaphosphate was added to the solution while stirring. After being stirred for 2 h, the suspension was left to stand for 20 min at room temperature. Thus, the impurities were precipitated in the bottom and were removed by filtration. To obtain the resultant HNTs, the upper solution was collected and separated by centrifugation; then the sample was freeze-dried overnight. Labeling of HNTs with FITC was performed as reported previously [28].

2.4. Microscopy Imaging

2.4.1. Scanning Electron Microscopy (SEM). SEM micrographs were obtained with a Quanta 200 FEG field emission scanning electron microscope (FEI, Eindhoven, Netherlands). Nanotube samples were applied to a metal wafer. After being dried overnight at room temperature, the sample was observed at an operating voltage of 15.0 KV.

2.4.2. Transmission Electron Microscopy (TEM). A Tecnai 12 Transmission Electron Microscope (FEI, Eindhoven, Netherlands) which was equipped with a Megaview III CCD camera and analysis camera control software (Olympus) was used to record images of HNTs. The samples were dropped onto carbon-coated 300-mesh copper grids and then images were recorded at an operating voltage of 120 KV.

2.4.3. Confocal Microscopy. Confocal micrographs were taken with a spinning-disk confocal microscope (Andor Revolution XD), which is equipped with an EMCCD (Andor iXon DV885K) and a 100x objective. Both the Z scan and XY scans were obtained to observe the internalization of HNTs inside cells.

2.5. In Vitro Degradation Test. HNTs were incubated at 37°C in 40 mL solution of phosphate-buffered saline (PBS) or in normal saline as a negative control. Each solution contained an equivalent (5 mg) mass of HNTs. At certain pH and designated time points, groups of samples were collected for inductively coupled plasma (ICP) emission spectral analysis to detect the content of silicon and aluminum in the solution.

2.6. Hemocompatibility Evaluation. All procedures concerning animal usage were reviewed and approved by the ethical committee of Wuhan University School of Medicine (Supplementary Figures S1 and S2 in Supplementary Material available online at http://dx.doi.org/10.1155/2015/685323).

2.6.1. Hemolysis Rate Test. Fresh rabbit blood was collected for standard hemolysis analysis. The fresh blood was added to anticoagulant and mixed with sterilized physiological saline at a ratio of 4 : 5. Here, sterilized physiological saline was used as the negative control and distilled water as the positive control. 0.2 mL of extraction medium of each sample was incubated in a 37°C water bath for an hour. Next, each tube was centrifuged and then the absorbance of the supernatant was recorded at a wave length of 545 nm. The hemolysis ratio was calculated as follows:

$$\mathrm{HR}\,(\%) = \frac{D_t - D_{\mathrm{nc}}}{D_{\mathrm{pc}} - D_{\mathrm{nc}}} \times 100\%, \quad (1)$$

where HR is hemolysis ration and D_t, D_{nc}, and D_{pc} are absorbance of samples, negative controls, and positive controls, respectively.

2.6.2. Plasma Clotting Activity Assay. Recalcification time was conducted as stated by Condrea et al. [29]. Fresh rabbit blood was mixed with 0.11 M Tri-sodium citrate in the ratio 1 : 9. The mixture was centrifuged at 3000 rpm for 20 min. The supernatant was used as platelet poor plasma (PPP). Six samples ranging from 10 to 200 μg/mL were added to the prewarmed PPP and incubated for one minute at 37°C. The clot formation was initiated by adding 0.25 M $CaCl_2$, and the time taken for visible clot to appear was recorded. For control experiments, saline solution (0.9% NaCl) alone was added instead of the enzyme source.

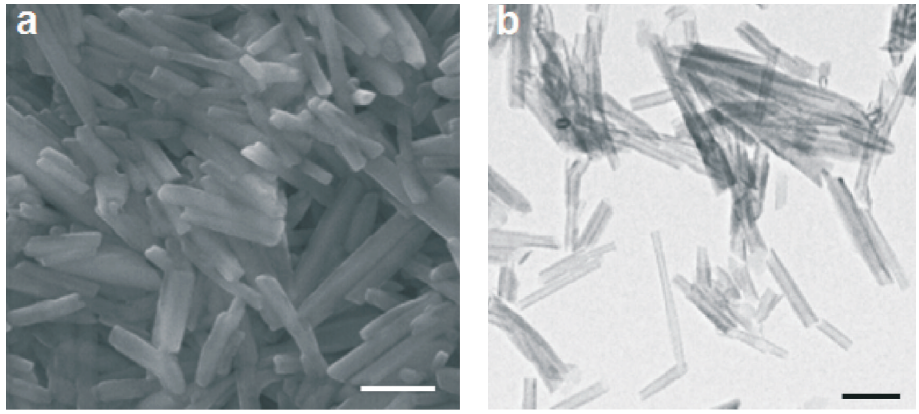

(a) (b)

Figure 1: SEM images ((a) scale bar: 500 nm) and TEM ((b) scale bar: 200 nm) photos of HNTs.

2.6.3. Platelet Activation. Fresh rabbit blood was collected in a tube preloaded with anticoagulant (3.8% (w/v) citrate sodium). Then the whole blood was centrifuged at 1000 rpm for 10 min at 4°C to obtain the platelet-rich plasma (PRP). HNTs were dispersed in PRP in different concentrations (from 10 to 200 μg/mL) and then incubated in 37°C water bath for 1 h. After incubation, samples were washed with DI water twice and then fixed with glutaraldehyde and imaged under SEM. A fresh blood sample without contact with HNTs was used as negative control.

2.7. Cytotoxicity Assays

2.7.1. Cell Viability. A cell count kit-8 (CCK-8 Beyotime, China) was employed in the cytotoxicity test. After A549 cells were incubated with various concentration of HNTs (from 10 to 200 μg/mL) for 24, 48, and 72 h, the original culture medium was replaced by 200 μL 10% FBS MEM medium containing 20 μL CCK-8. After 3 h at 37°C, the formazan solution were taken from each sample. The absorbances at 450 nm were determined using a BioTek Elx800 UV-vis spectrophotometer. DMEM containing 10% CCK-8 was used as a control.

2.7.2. TUNEL Assay. Apoptotic A549 cells were measured by using TUNEL method to label 3′-end of fragmented DNA. A549 cells treated with different concentration of HNTs (from 10 to 200 μg/mL) were fixed with 4% paraformaldehyde in PBS for 1 h at room temperature. Then A549 cells were washed with PBS once. After being permeabilized by 0.1% Triton X-100 for FITC labeling of the fragmented DNA, A549 cells were added to 50 mL of the TUNEL assay solution and then were incubated at 37°C for 60 min in the dark. Then, A549 cells were mounted on the slide and imaged under a fluorescent microscopy at 488 nm excitation and 530 nm emission. The percent of TUNEL-positive cells was quantified as follows:

$$\text{TUNEL-positive cells (\%)} = 100\left(\frac{\text{apoptotic cells}}{\text{total cells}}\right). \quad (2)$$

2.8. Statistical Analysis. All quantitative results were performed by using one-way ANOVA. Data were expressed as the mean ± SD. Two-tailed unpaired Student's t-test was used to calculate p values. A value of $p < 0.05$ indicates significant difference.

3. Results and Discussion

3.1. Characterization. Previous toxicological studies have suggested that minute particle size and specific shape of nanoparticle may cause adverse effects in the process of interacting with cells [30, 31]. Thus, SEM and TEM images were carried out to characterize the morphology and detailed structure of HNTs we used. As illustrated in Figure 1(a), the majority of the nanotubes were presented with cylindrical shape, which have clean and smooth walls. As displayed in TEM image in Figure 1(b), the size of purified HNTs with open-ended tubular morphology was about 0.2–1 μm in length and 20–50 nm in diameter while the inner diameter was found to be 10–20 nm. One can see that some nanotubes were not tightly rolled and interlaced with each other.

Also, the degradation characteristics of HNTs were investigated in vitro. It is shown in Figure 2 that silicon and aluminum ions concentrations in PBS pH 1.0 and 8.3 solutions were slowly increased with time accumulation from 15 to 180 days. HNTs degradation rate was too slow to reach the final stable balance of dissociation equilibrium reaction at 180 days. The results suggested that HNTs are biodegradable under certain environmental conditions but at a very low degradation rate. Strong acidic conditions prompt the degradation rate of HNTs more significant than in weak alkaline conditions (silicon and aluminum elements mass % of degraded HNTs has been given in Supplementary Figure S3). Although the aluminosilicate chemical structure should be nonbiodegradable, the increase in specific surface area of HNTs nanoparticles can cause the enhancement of ionic dissolution [32]. Furthermore, the degradation rate is in a higher level under strong acidic conditions, which may be because of the increase of silicon or aluminum ions and hydrogen ions in solutions that can help form a more stable

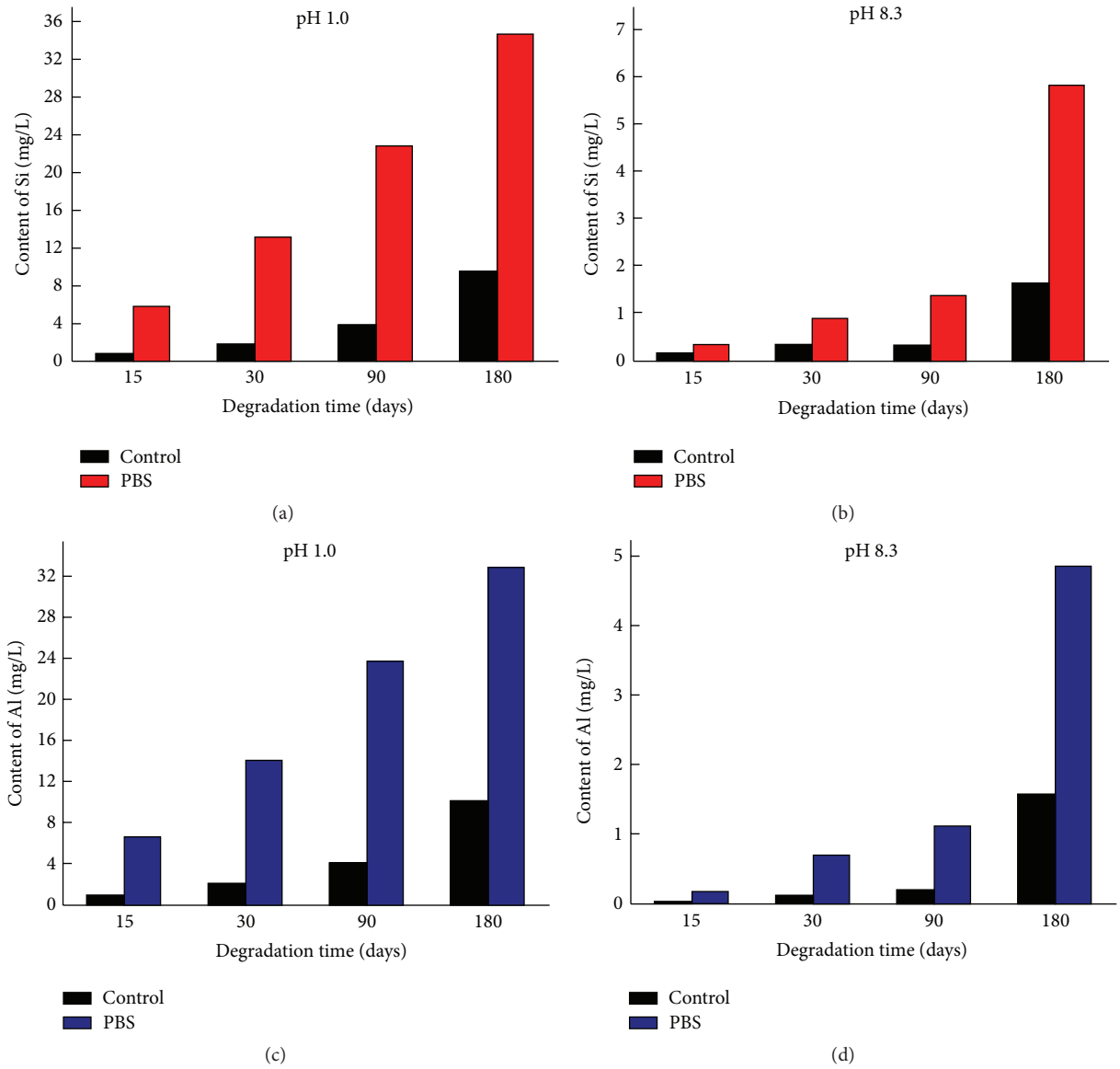

Figure 2: In vitro degradation characteristics of HNTs in PBS, pH 1.0 (a, c) and pH 8.3 (b, d) at 37°C. Normal saline at the same pH value with PBS as a negative control.

colloidal dispersion of HNTs. These results have potential to bring promising application prospect of HNTs in the field of drug delivery.

3.2. Intracellular Distribution. Nanoparticles mainly enter our body via the respiratory route and alveolar epithelial cells are the first front of interaction with the inhaled nanoparticles. Therefore, A549 cell is selected as a model system of airborne particle exposure to investigate halloysite toxicity. Firstly, the interaction of fluorescently labeled HNTs with A549 cells was observed under confocal microscope (Supplementary Figure S4). The cells were incubated with FITC-labeled HNTs, and then DiD and Hoechst 33342 were used to label the membrane and the nucleus of the treated cells. Orthogonal view of the live cells demonstrated the uptake of HNTs by A549 cells (Figure 3). The fluorescence signals appeared in a specific region inside the cell and showed a heterogeneous distribution in the cytoplasm. Similarly, colocalization of FITC-labeled HNTs and stained nucleus was also imaged. The results suggested that FITC signals appeared in the surrounding area of the cell nucleus but were not observed inside the cell nucleus even for a longer incubation time, illustrating that the HNTs could not enter into the cell nucleus.

3.3. Hemocompatibility. The blood compatibility is the prerequisite of nanoparticle for intravascular drug delivery. In our study, we performed three hemocompatibility tests: hemolysis ratio test, plasma clotting activity assay, and platelet activation test. Hemolysis study showed the stability of red blood cell when contacting with a foreign object. If the hemolysis rate is below 5%, medical materials were

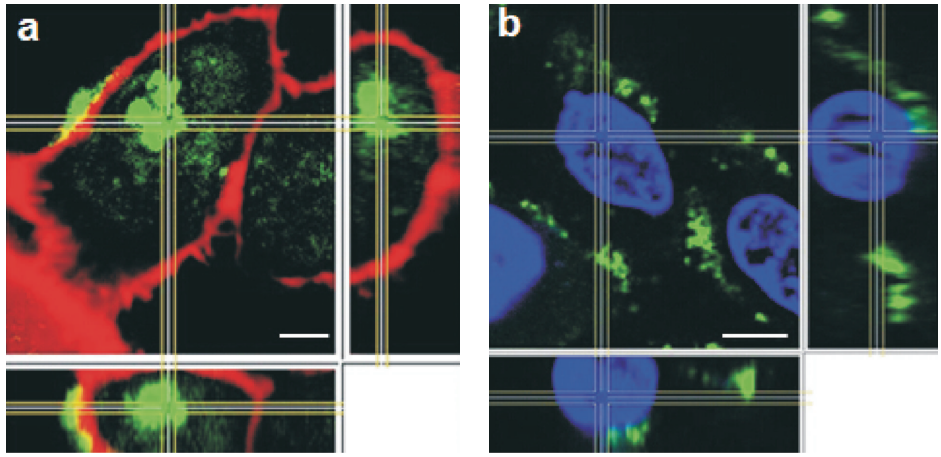

(a) (b)

Figure 3: Confocal microscope image of internalized HNTs in live cells. (a) Colocalization of FITC-labeled HNTs with cell membrane. (b) Colocalization of FITC-labeled HNTs with cell nucleus. Scale bar: 5 μm.

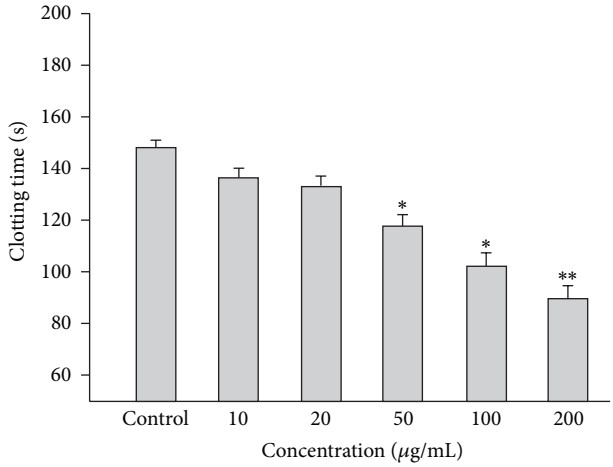

Figure 4: Recalcification assay of HNTs on citrate rabbit plasma. The data are presented as the means ± SEM. $^{*}p < 0.01$ versus control group. $^{**}p < 0.001$ versus control group.

Table 1: Hemolysis caused by different HNTs concentration.

Samples	Optical density at 545 nm	HR (%)
Normal saline (negative control)	0.0268 ± 0.0020	0
Distilled water (positive control)	0.588 ± 0.0103	100
10 μg/mL	0.0455 ± 0.0040	3.33
20 μg/mL	0.0485 ± 0.0031	3.86
50 μg/mL	0.0472 ± 0.0045	3.63
100 μg/mL	0.0491 ± 0.0066	3.97
200 μg/mL	0.0495 ± 0.0042	4.04

Standard deviation is calculated from three samples.

considered as nonhemolysis according to national biological safety. The hemolysis ratio of HNTs at various concentrations was tested in vitro by a direct contact method (Table 1). The results of all samples were all less than 5%, conforming to the national biological material hemolysis rate security specified requirements.

In order to check the coagulant (pro/anti)activity of HNTs, the plasma recalcification time was investigated (Figure 4). The results showed that HNTs reduced the plasma recalcification time in a dose-dependent manner. The clotting time reduced slightly in the concentration lower than 20 μg/mL and showed no significant difference, suggesting no obvious procoagulant effect of HNTs. With increasing HNTs concentration from 50 μg/mL to 200 μg/mL, there was a clear decrease in clotting time ($p < 0.01$), which demonstrated that HNTs exhibited procoagulant activity on recalcification with citrated plasma.

It has been reported that the ability of materials to support blood coagulation is mainly attributed to the promoted platelet activation of this material [33]. Here, the platelet activation was examined. Figure 5 shows the scanning electron micrographs of platelets after contact with different dose of HNTs. Almost no platelet activation occurred in the control sample and low concentration range (10 μg/mL). In contrast, many platelets aggregated together and had developed pseudopodia in high concentration group, which proved that HNTs could active platelet in vitro. Actually, carbon nanotubes (CNT), another tubular structure nanomaterial, have demonstrated a similar ability of HNTs to support blood coagulation [34, 35]. Indeed, nanomaterials react to the platelet activation in clearly different ways. Since the cylindrical structure of nanotubes appear to promote platelet contact with each other and induce aggregation, while nanospheres do not, we suggest that the tubular structure of HNTs may play a role in aggregating and activating of platelet. Since the nanoparticle surface properties may underlie their ability to aggregate platelets [34], the combination of biomolecules and HNTs will give rise to the idea that there is a possibility of finding a feasible way to alter the properties of HNTs [36] and thus to improve its hemocompatibility.

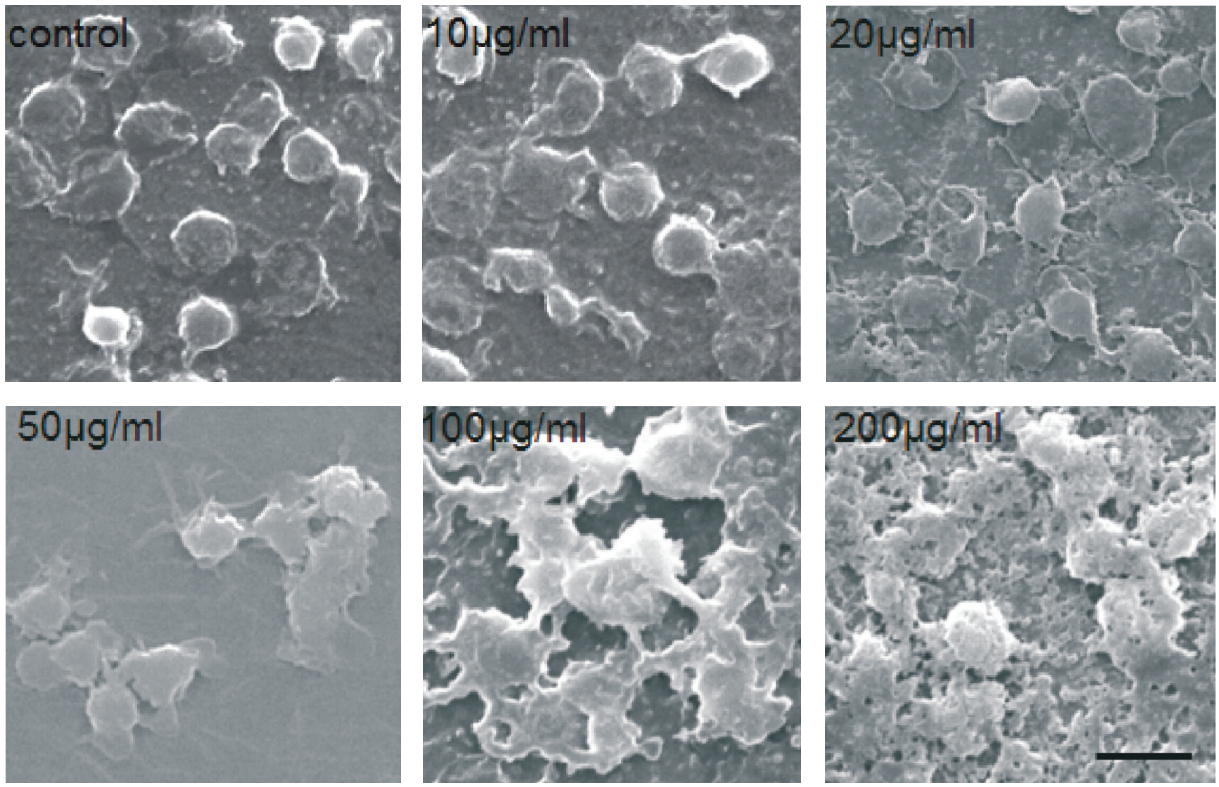

Figure 5: SEM images of platelet after contact with various HNTs concentration. Scale bar: 5 μm.

3.4. Cytotoxicity Test. The elucidation of the toxicity of HNTs towards human cells is a crucially important topic associated with the biomedical application of the nanoparticles. Here, we carefully investigated the toxicity profiles of HNTs on A549 cells by employing CCK-8 test and TUNEL assay. CCK-8 tests were performed at different time intervals (24 to 72 h) and at different concentrations (from 10 μg/mL to 200 μg/mL). HNTs showed almost nontoxicity to the viability of A549 cells up to a dose of 50 μg/mL (Figure 6). At a higher dose, HNTs exhibited obviously inhibition in a dose-dependent manner. The cell viability was maintained at 75% for HNTs concentration up to 100 μg/mL at 72 h. With an increasing HNTs concentration to 200 μg/mL, it shows a significant vitality reduction. These data demonstrates that HNTs suggest a high biocompatibility for A549 cells at a lower concentration (<100 μg/mL).

Then, TUNEL assay was employed to detect A549 cells containing massive DNA breaking, a feature of late apoptosis (Figure 7). Cells were exposed to different concentrations of HNTs for 12 h. In the low concentration range (<20 μg/mL), no statistically significant increase of positive cells for DNA breakage was measured compared to control group. But when the concentration of HNTs was up to 50 μg/mL, many positive cells can be seen clearly. With an increasing concentration, there was a distinctive increase of positive cell number.

The toxicity of HNTs had been investigated towards living organisms in different levels. According to Fakhrullina et al., the pristine HNTs within 1 mg/mL will not be capable of causing severe toxicity effect on the organism of the nematodes [22]. Besides, HNTs were shown to have little toxicity to *Escherichia coli* bacteria [37] and almost nontoxicity to yeast cells [38]. However, the investigations above did not reveal the aspect of potential cytotoxicity which has become a significant point related to the biological consequence of HNTs.

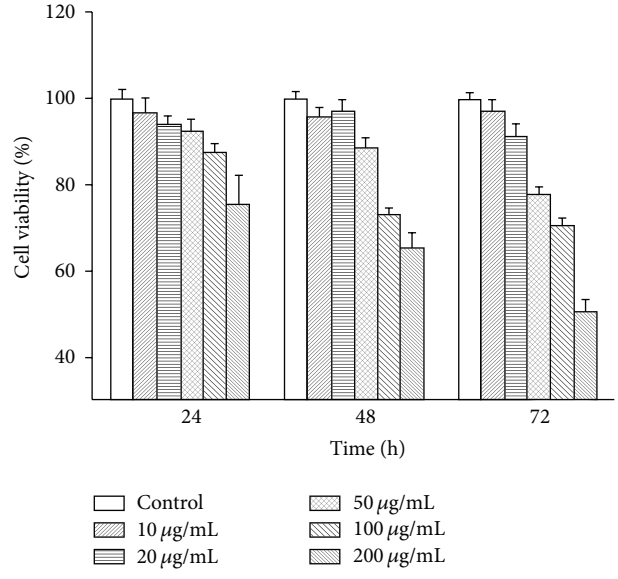

Figure 6: CCK-8 test of HNTs in A549 cells. Percent cell viability versus time at different HNTs concentration.

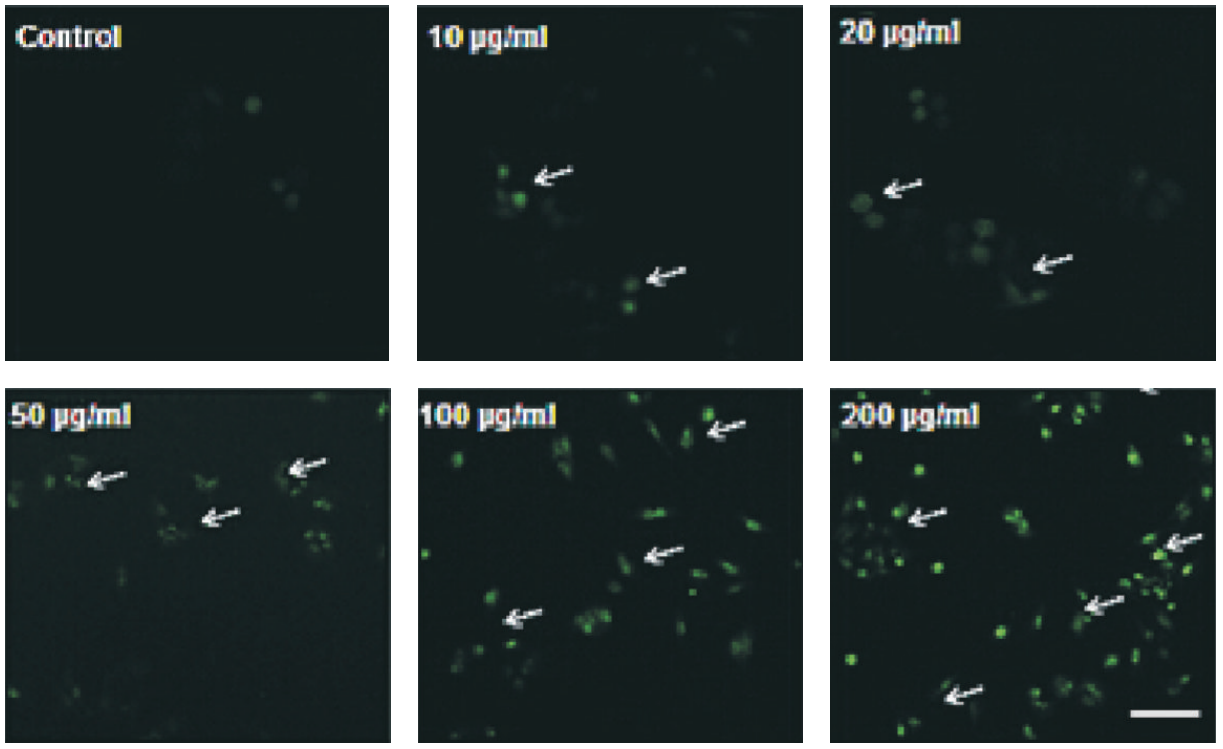

(a)

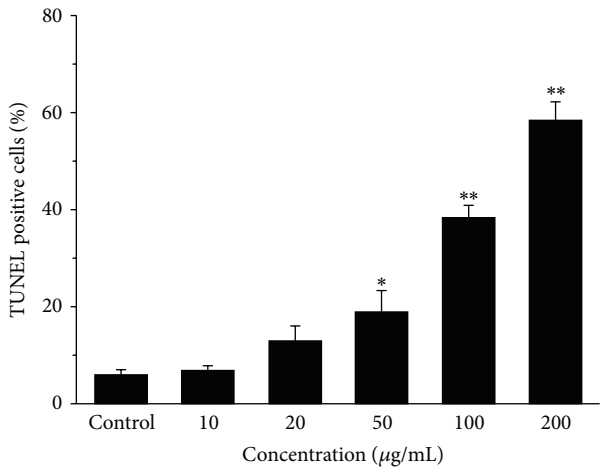

(b)

Figure 7: TUNEL analysis of different HNTs concentration. (a) Fluorescent image of cells treated with TUNEL staining. Scale bar: 50 μm. (b) Quantitative analysis of TUNEL-positive cells content in different groups. The data are presented as the means ± SEM. $^{*}p < 0.01$ versus control group. $^{**}p < 0.001$ versus control group.

In our work, the extent of cytotoxicity of HNTs on A549 cells was detected at cellular level. CCK-8 results showed that HNTs exhibit slight toxicity effects on the proliferation up to 100 μg/mL. But the TUNEL assay suggested that HNTs will cause DNA breakage from 50 μg/mL, which means that HNTs may cause latent toxicity effects on A549 cells in a concentration lower than 100 μg/mL. The interaction of HNTs with cell surface and reactive oxygen generation may be the main reasons to give rise to toxicity [38].

4. Conclusion

In brief, internalization localization of HNTs inside A549 cells was observed under confocal microscope and both the hemocompatibility and cytotoxicity of HNTs were evaluated in this work. The results show that HNTs can readily internalize into live cells and aggregate together around nucleus region. Hemolysis ratio test showed nonhemolysis of HNTs. Recalcification time demonstrated that HNTs reduced the

plasma recalcification time in a dose-dependent manner, which means that HNTs exhibited procoagulant activity with citrated plasma. Platelet activation micrographs imaged with SEM proved that HNTs could active platelet in vitro. Both CCK-8 test and TUNEL test suggested that HNTs exhibit good cell compatibility in low concentration range. All these results provide useful guide to clinical research and biomedical application of HNTs.

Conflict of Interests

The authors declare that there is no conflict of interests regarding the publication of this paper.

Acknowledgments

This work was financially supported by the fund of Science and Technology Bureau of Wuhan City (201260523188) and National Science and Technology Major Project of the Ministry of Science and Technology of China (2011ZX-05059-004).

References

[1] G. Tarì, I. Bobos, C. S. F. Gomes, and J. M. F. Ferreira, "Modification of surface charge properties during kaolinite to halloysite-7Å transformation," *Journal of Colloid and Interface Science*, vol. 210, no. 2, pp. 360–366, 1999.

[2] E. Joussein, S. Petit, J. Churchman, B. Theng, D. Righi, and B. Delvaux, "Halloysite clay minerals—a review," *Clay Minerals*, vol. 40, no. 4, pp. 383–426, 2005.

[3] S. R. Levis and P. B. Deasy, "Characterisation of halloysite for use as a microtubular drug delivery system," *International Journal of Pharmaceutics*, vol. 243, no. 1-2, pp. 125–134, 2002.

[4] V. Vergaro, Y. M. Lvov, and S. Leporatti, "Halloysite clay nanotubes for resveratrol delivery to cancer cells," *Macromolecular Bioscience*, vol. 12, no. 9, pp. 1265–1271, 2012.

[5] M. Remškar, "Inorganic nanotubes," *Advanced Materials*, vol. 16, no. 17, pp. 1497–1504, 2004.

[6] P. Yuan, P. D. Southon, Z. Liu et al., "Functionalization of halloysite clay nanotubes by grafting with γ-aminopropyltriethoxysilane," *Journal of Physical Chemistry C*, vol. 112, no. 40, pp. 15742–15751, 2008.

[7] N. G. Veerabadran, R. R. Price, and Y. M. Lvov, "Clay nanotubes for encapsulation and sustained release of drugs," *Nano*, vol. 2, no. 2, pp. 115–120, 2007.

[8] M. Liu, W. Li, J. Rong, and C. Zhou, "Novel polymer nanocomposite hydrogel with natural clay nanotubes," *Colloid and Polymer Science*, vol. 290, no. 10, pp. 895–905, 2012.

[9] S. Rooj, A. Das, V. Thakur, R. N. Mahaling, A. K. Bhowmick, and G. Heinrich, "Preparation and properties of natural nanocomposites based on natural rubber and naturally occurring halloysite nanotubes," *Materials & Design*, vol. 31, no. 4, pp. 2151–2156, 2010.

[10] P. Pasbakhsh, H. Ismail, M. N. A. Fauzi, and A. A. Bakar, "EPDM/modified halloysite nanocomposites," *Applied Clay Science*, vol. 48, no. 3, pp. 405–413, 2010.

[11] C. Li, J. Liu, X. Qu, and Z. Yang, "A general synthesis approach toward halloysite-based composite nanotube," *Journal of Applied Polymer Science*, vol. 112, no. 5, pp. 2647–2655, 2009.

[12] H. Ismail, P. Pasbakhsh, M. N. Ahmad Fauzi, and A. Abu Bakar, "The effect of halloysite nanotubes as a novel nanofiller on curing behaviour, mechanical and microstructural properties of ethylene propylene diene monomer (EPDM) nanocomposites," *Polymer—Plastics Technology and Engineering*, vol. 48, no. 3, pp. 313–323, 2009.

[13] M. R. Dzamukova, E. A. Naumenko, Y. M. Lvov, and R. F. Fakhrullin, "Enzyme-activated intracellular drug delivery with tubule clay nanoformulation," *Scientific Reports*, vol. 5, Article ID 10560, 2015.

[14] R. T. De Silva, P. Pasbakhsh, K. L. Goh, S.-P. Chai, and H. Ismail, "Physico-chemical characterisation of chitosan/halloysite composite membranes," *Polymer Testing*, vol. 32, no. 2, pp. 265–271, 2013.

[15] G. Cavallaro, G. Lazzara, and S. Milioto, "Dispersions of nanoclays of different shapes into aqueous and solid biopolymeric matrices. Extended physicochemical study," *Langmuir*, vol. 27, no. 3, pp. 1158–1167, 2011.

[16] G. Cavallaro, D. I. Donato, G. Lazzara, and S. Milioto, "Films of halloysite nanotubes sandwiched between two layers of biopolymer: from the morphology to the dielectric, thermal, transparency, and wettability properties," *Journal of Physical Chemistry C*, vol. 115, no. 42, pp. 20491–20498, 2011.

[17] D. G. Shchukin, S. V. Lamaka, K. A. Yasakau, M. L. Zheludkevich, M. G. S. Ferreira, and H. Möhwald, "Active anticorrosion coatings with halloysite nanocontainers," *Journal of Physical Chemistry C*, vol. 112, no. 4, pp. 958–964, 2008.

[18] D. G. Shchukin and H. Möhwald, "Surface-engineered nanocontainers for entrapment of corrosion inhibitors," *Advanced Functional Materials*, vol. 17, no. 9, pp. 1451–1458, 2007.

[19] D. Fix, D. V. Andreeva, Y. M. Lvov, D. G. Shchukin, and H. Möhwald, "Application of inhibitor-loaded halloysite nanotubes in active anti-corrosive coatings," *Advanced Functional Materials*, vol. 19, no. 11, pp. 1720–1727, 2009.

[20] E. Abdullayev, R. Price, D. Shchukin, and Y. Lvov, "Halloysite tubes as nanocontainers for anticorrosion coating with benzotriazole," *ACS Applied Materials & Interfaces*, vol. 1, no. 7, pp. 1437–1443, 2009.

[21] J. Xue, Y. Niu, M. Gong et al., "Electrospun microfiber membranes embedded with drug-loaded clay nanotubes for sustained antimicrobial protection," *ACS Nano*, vol. 9, no. 2, pp. 1600–1612, 2015.

[22] G. I. Fakhrullina, F. S. Akhatova, Y. M. Lvov, and R. F. Fakhrullin, "Toxicity of halloysite clay nanotubes *in vivo*: a *Caenorhabditis elegans* study," *Environmental Science: Nano*, vol. 2, no. 1, pp. 54–59, 2015.

[23] M. Liu, C. Wu, Y. Jiao, S. Xiong, and C. Zhou, "Chitosan—halloysite nanotubes nanocomposite scaffolds for tissue engineering," *Journal of Materials Chemistry B*, vol. 1, no. 15, pp. 2078–2089, 2013.

[24] Y. M. Lvov, A. Aerov, and R. Fakhrullin, "Clay nanotube encapsulation for functional biocomposites," *Advances in Colloid and Interface Science*, vol. 207, no. 1, pp. 189–198, 2014.

[25] A. D. Hughes and M. R. King, "Use of naturally occurring halloysite nanotubes for enhanced capture of flowing cells," *Langmuir*, vol. 26, no. 14, pp. 12155–12164, 2010.

[26] B.-H. Luo, C.-E. Hsu, J.-H. Li et al., "Nano-composite of poly(L-lactide) and halloysite nanotubes surface-grafted with L-lactide oligomer under microwave irradiation," *Journal of Biomedical Nanotechnology*, vol. 9, no. 4, pp. 649–658, 2013.

[27] W. O. Yah, A. Takahara, and Y. M. Lvov, "Selective modification of halloysite lumen with octadecylphosphonic acid: new inorganic tubular micelle," *Journal of the American Chemical Society*, vol. 134, no. 3, pp. 1853–1859, 2012.

[28] V. Vergaro, E. Abdullayev, Y. M. Lvov et al., "Cytocompatibility and uptake of halloysite clay nanotubes," *Biomacromolecules*, vol. 11, no. 3, pp. 820–826, 2010.

[29] E. Condrea, C. C. Yang, and P. Rosenberg, "Anticoagulant activity and plasma phosphatidylserine hydrolysis by snake venom phospholipases A2," *Thrombosis and Haemostasis*, vol. 49, no. 2, p. 151, 1983.

[30] M. D. Chavanpatil, A. Khdair, and J. Panyam, "Nanoparticles for cellular drug delivery: mechanisms and factors influencing delivery," *Journal of Nanoscience and Nanotechnology*, vol. 6, no. 9-10, pp. 2651–2663, 2006.

[31] J. Rejman, V. Oberle, I. S. Zuhorn, and D. Hoekstra, "Size-dependent internalization of particles via the pathways of clathrin-and caveolae-mediated endocytosis," *Biochemical Journal*, vol. 377, no. 1, pp. 159–169, 2004.

[32] F. Watari, N. Takashi, A. Yokoyama et al., "Material nanosizing effect on living organisms: non-specific, biointeractive, physical size effects," *Journal of the Royal Society Interface*, no. 6, pp. S371–S388, 2009.

[33] T.-C. Chou, E. Fu, C.-J. Wu, and J.-H. Yeh, "Chitosan enhances platelet adhesion and aggregation," *Biochemical and Biophysical Research Communications*, vol. 302, no. 3, pp. 480–483, 2003.

[34] A. Radomski, P. Jurasz, D. Alonso-Escolano et al., "Nanoparticle-induced platelet aggregation and vascular thrombosis," *British Journal of Pharmacology*, vol. 146, no. 6, pp. 882–893, 2005.

[35] Y. Niwa and N. Iwai, "Nanomaterials induce oxidized low-density lipoprotein cellular uptake in macrophages and platelet aggregation," *Circulation Journal*, vol. 71, no. 3, pp. 437–444, 2007.

[36] Y. M. Lvov and E. Abdullayev, "Functional polymer-clay nanotube composites with sustained release of chemical agents," *Progress in Polymer Science*, vol. 38, no. 10-11, pp. 1690–1719, 2013.

[37] H.-J. Choi, T. J. Stazak Jr., and C. D. Montemagno, "Surface-dependent cytotoxicity on bacteria as a model for environmental stress of halloysite nanotubes," *Journal of Nanoparticle Research*, vol. 15, no. 10, article 2008, 2013.

[38] S. A. Konnova, I. R. Sharipova, T. A. Demina et al., "Biomimetic cell-mediated three-dimensional assembly of halloysite nanotubes," *Chemical Communications*, vol. 49, no. 39, pp. 4208–4210, 2013.